The EMBO Journal vol.12 no.9 pp.3587-3598, 1993

Poliovirus RNA synthesis utilizes an RNP complex formed around the 5′-end of viral RNA

Raul Andino[1], Gabrielle E.Rieckhof[2], Philip L.Achacoso and David Baltimore[3]

The Rockefeller University, 1230 York Avenue, New York, NY 10021, USA

[1]Present address: Gladstone Institute of Virology and Immunology, and Department of Microbiology and Immunology, University of California, San Francisco, PO Box 419100, San Francisco, CA 94141, USA

[2]Present address: College of Physicians and Surgeons of Columbia University, 701 West 168 Street, New York, NY 10032, USA

[3]Corresponding author

Communicated by D.Baltimore

The structure of a ribonucleoprotein complex formed at the 5′-end of poliovirus RNA was investigated. This complex involves the first 90 nucleotides of poliovirus genome which fold into a cloverleaf-like structure and interact with both uncleaved 3CD, the viral protease-polymerase precursor, and a 36 kDa ribosome-associated cellular protein. The cellular protein is required for complex formation and interacts with unpaired bases in one stem–loop of the cloverleaf RNA. Amino acids within the 3C protease which are important for RNA binding were identified by site-directed mutagenesis and the crystal structure of a related protease was used to model the RNA binding domain within the viral 3CD protein. The physiologic importance of the ribonucleoprotein complex is suggested by the finding that mutations that disrupt complex formation abolish RNA replication but do not affect RNA translation or stability. Based on these structural and functional findings we propose a model for the initiation of poliovirus RNA synthesis where an initiation complex consisting of 3CD, a cellular protein, and the 5′-end of the positive strand RNA catalyzes *in trans* the initiation of synthesis of new positive stranded RNA.

Key words: initiation complex/poliovirus/protease-polymerase/ribonucleoprotein/RNA synthesis

Introduction

Poliovirus RNA replication follows a strategy common to all positive-stranded lytic RNA viruses: the viral genome is transcribed into a complementary RNA (negative strand), which in turn is used as a template to synthesize new strands of genomic RNA. The detailed mechanisms have yet to be worked out. A virus-encoded RNA-dependent RNA polymerase ($3D^{pol}$) is thought to catalyze the synthesis of both strands. However, because $3D^{pol}$ is a primer-dependent enzyme, several other viral factors (proteins or RNA structures), as well as cellular factors, are likely to be involved in the RNA initiation process. Genetic analysis has implicated most of the non-structural viral proteins in RNA synthesis (Bernstein *et al.*, 1986; Kuhn *et al.*, 1988; Li and Baltimore, 1988; Burns *et al.*, 1989; Giachetti and Semler, 1991; Kirkegaard, 1992).

Two functional regions have been defined within the long and well-conserved 5′ non-coding region of poliovirus genomic RNA: a long element involved in cap-independent initiation of translation and a shorter 5′-terminal element involved in viral RNA replication (Sonenberg, 1987; Pelletier *et al.*, 1988; Trono *et al.*, 1988). We have recently demonstrated that the 5′-most 100 nucleotides of the domain that is involved in RNA synthesis fold into a cloverleaf-like structure. This structure is physiologically required in the viral genomic RNA, but not in the complementary negative strand. It binds a cellular factor, the major viral proteinase ($3C^{pro}$) and the viral RNA polymerase ($3D^{pol}$). This ribonucleoprotein complex appears to be required for positive RNA synthesis but is dispensable for negative strand synthesis, suggesting that the complex may play a fundamental role in plus strand synthesis (Andino *et al.*, 1990a).

By further analyzing this complex we have discovered that 3CD, the uncleaved precursor of $3C^{pro}$ and $3D^{pol}$, is the viral component of the 5′-end ribonucleoprotein complex, that a 36 kDa ribosome-associated cellular protein is required for complex formation, and that the cellular factor interacts directly with one RNA stem–loop. Also, we have shown that poliovirus protease ($3C^{pro}$) is itself an RNA binding protein. Mutagenesis and model building suggest that several amino acids in the $3C^{pro}$ protease, separated in the primary sequence, may form part of an RNA binding domain located on a side of the protein opposite to the proteolytically active site. Finally, using a new reporter system based on a chimeric subgenomic replicon, we confirm that the RNP complex is necessary for poliovirus RNA replication. We suggest a role for the 5′-RNP complex of initiating *in trans* synthesis of new plus strands.

Results

Identifying viral proteins in the RNP-B complex

The 5′-most 90 nucleotides of poliovirus genomic RNA fold into a cloverleaf-like structure that interacts specifically with proteins present in extracts prepared from poliovirus-infected cells to form a ribonucleoprotein complex (referred to as RNP-B). The viral protease ($3C^{pro}$) and the viral polymerase ($3D^{pol}$) can be detected in the RNP-B complex by immunological methods, suggesting that these two proteins are part of the complex (Andino *et al.*, 1990a). Because $3C^{pro}$ and $3D^{pol}$ accumulate in poliovirus-infected cells both as independent polypeptides and in an uncleaved form, 3CD, the precise nature of the viral proteins in the RNP-B was examined.

To investigate which viral proteins were in the complex, ^{35}S-labeled extracts prepared from poliovirus-infected HeLa cells were incubated with unlabeled cloverleaf RNA to form complex RNP-B. The resulting complex was purified by non-denaturing polyacrylamide gel electrophoresis and the

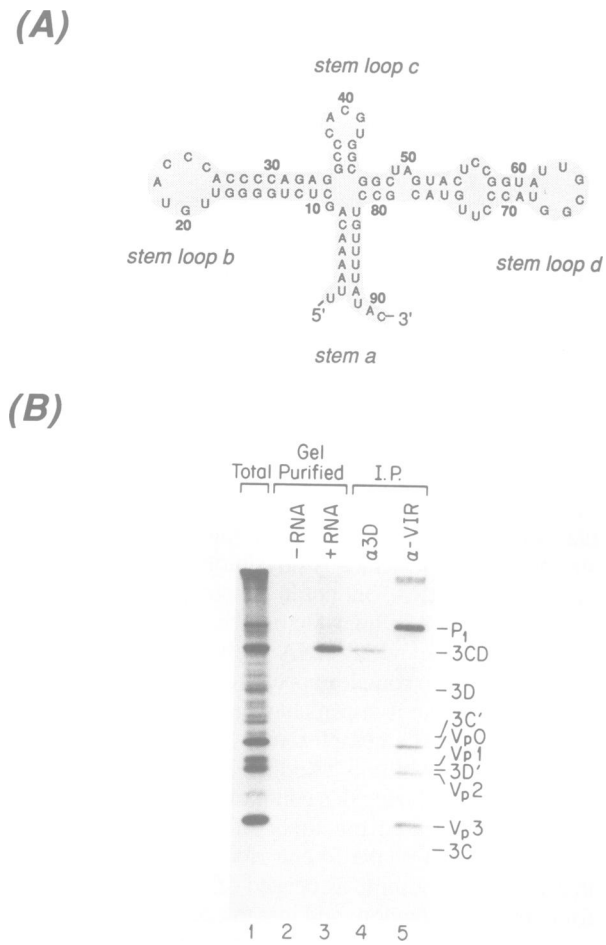

Fig. 1. The viral components of the ribonucleoprotein complex B (RNP-B) are a cloverleaf RNA and the uncleaved precursor 3CD. (**A**) Secondary structure of the first 91 nucleotides at the 5′-end of the viral genome. The verified cloverleaf structure of the 5′-most 91 nucleotides of the poliovirus genomic RNA is shown. The structure can be subdivided into four domains, here named stem a (nucleotides 2–8 and 82–88), stem–loop b (10–34), stem–loop c (35–45) and stem–loop d (51–78). (**B**) SDS–polyacrylamide gel analysis of the ^{35}S-labeled viral proteins that interact with cloverleaf RNA. Poliovirus-infected HeLa cells were labeled with [^{35}S]methionine, 25 μg of labeled cytoplasmic extracts were incubated with 5 μg unlabeled cloverleaf RNA (lane 3) or without specific RNA (lane 2), followed by electrophoresis through a non-denaturing polyacrylamide gel. Proteins were eluted by passive diffusion from the region of the gel corresponding to complex B, and analyzed by 10% SDS–PAGE. Lane 1, 1.0 μg of total HeLa cell cytoplasmic extract. For comparison, lanes 4 and 5 show products of an immunoprecipitation using, respectively, anti-3D^{pol} and anti-virion sera. The relative migration positions of poliovirus proteins are indicated.

[^{35}S]proteins that co-migrate with RNP-B were then analyzed by SDS–PAGE (Figure 1B). A single polypeptide with the same electrophoretic mobility as 3CD was specifically enriched in the purified material (Figure 1B, lane 3; compare with immunoprecipitated 3CD in lane 4). As a control, a binding reaction performed in the absence of cloverleaf RNA yielded no detectable 3CD migrating in the region of RNP-B (Figure 1B, lane 2).

To confirm the presence of the uncleaved 3CD in the complex, we expressed in *Escherichia coli* 3C^{pro}, 3D^{pol}, 3CD and a mutated 3CD with an alteration at the cleavage site between 3C^{pro} and 3D^{pol} (Gln182 to Asp) that largely eliminated the auto-proteolytic processing of the precursor 3CD (Figure 2A). Western blot analysis confirmed the expression of poliovirus proteins in the bacterial system (Figure 2B), and demonstrated that the point mutation at the junction of 3C^{pro} and 3D^{pol} in pT-3CD-N182 indeed abolished proteolytic processing of 3CD (Figure 2B, lanes 6 and 12). We then analyzed the ability of these bacterially expressed viral proteins to form RNP-B by electrophoretic mobility shift assays (EMSA). Suspecting that a cellular factor might be required for complex formation, the binding reaction was supplemented with extracts prepared from non-infected HeLa cells. The bacterial extracts containing non-poliovirus proteins (vector), 3C^{pro} (pT-3C), or 3D^{pol} (pT-3D) were unable to form complex RNP-B (Figure 2C, lanes 4, 5 and 6, respectively). Moreover, when 3C^{pro} and 3D^{pol}, expressed independently, were incubated together in the binding reaction, no RNP-B complex formation was detected (Figure 2C, lane 7). By contrast, *E.coli* extracts expressing 3CD formed a complex with an electrophoretic mobility identical to that of the RNP-B formed with proteins from poliovirus-infected HeLa cell extracts (Figure 2C, compare lanes 3 and 8). The mutant 3CD, that was virtually unable to be cleaved to 3C and 3D, formed the complex with an efficiency equal to that of wild-type 3CD (Figure 2C, lane 9). Furthermore, the complexes obtained using bacterially expressed 3CD behaved similarly to those from poliovirus-infected HeLa cell extracts in their sensitivity to SDS and proteinase K treatment and in binding specificity and affinity (data not shown). Finally, the identity of these complexes was confirmed by including anti-3D specific antiserum in the binding reactions which produced a 'super-shift' in the EMSA analysis (Figure 2C, lanes 10 and 11). These data indicate that the viral protein component of complex RNP-B is the uncleaved precursor 3CD and that its autoproteolytic processing reduces the affinity of the viral proteins for the RNA.

A cellular polypeptide of 36 kDa is required for RNP-B complex formation

To test if a cell host factor might be required for complex B formation, we analyzed the ability of 3CD produced in bacteria to form RNP-B in the absence or presence of uninfected HeLa cell extract. A complete binding reaction, containing bacterially expressed 3CD and uninfected HeLa cell extract, yielded a complex corresponding to RNP-B (Figure 3A, lane 6), but no such complex was produced by the same amount of 3CD when HeLa cell extract was not added (lane 3). Instead, a weak band which migrated slightly faster than RNP-B was observed (Figure 3A, lane 3 indicated as II), which was not evident without 3CD (lane 1), and presumably represents a weak interaction of 3CD with the cloverleaf RNA by itself. Therefore, complex B formation appears to depend on a cellular factor present in HeLa cell cytoplasmic extract. In addition, the faster electrophoretic mobility of complex II suggests that the cellular factor may actually form part of complex B.

To characterize the cellular component of the RNP-B further, we partially purified the cellular activity that enhances the formation of complex RNP-B. This activity appears to be significantly associated with ribosomes (30–40% of the total cytoplasmic activity); therefore we used this property as a part of our purification protocol. A ribosomal pellet was obtained by centrifugation of the HeLa cell cytoplasmic extract through a sucrose cushion, the

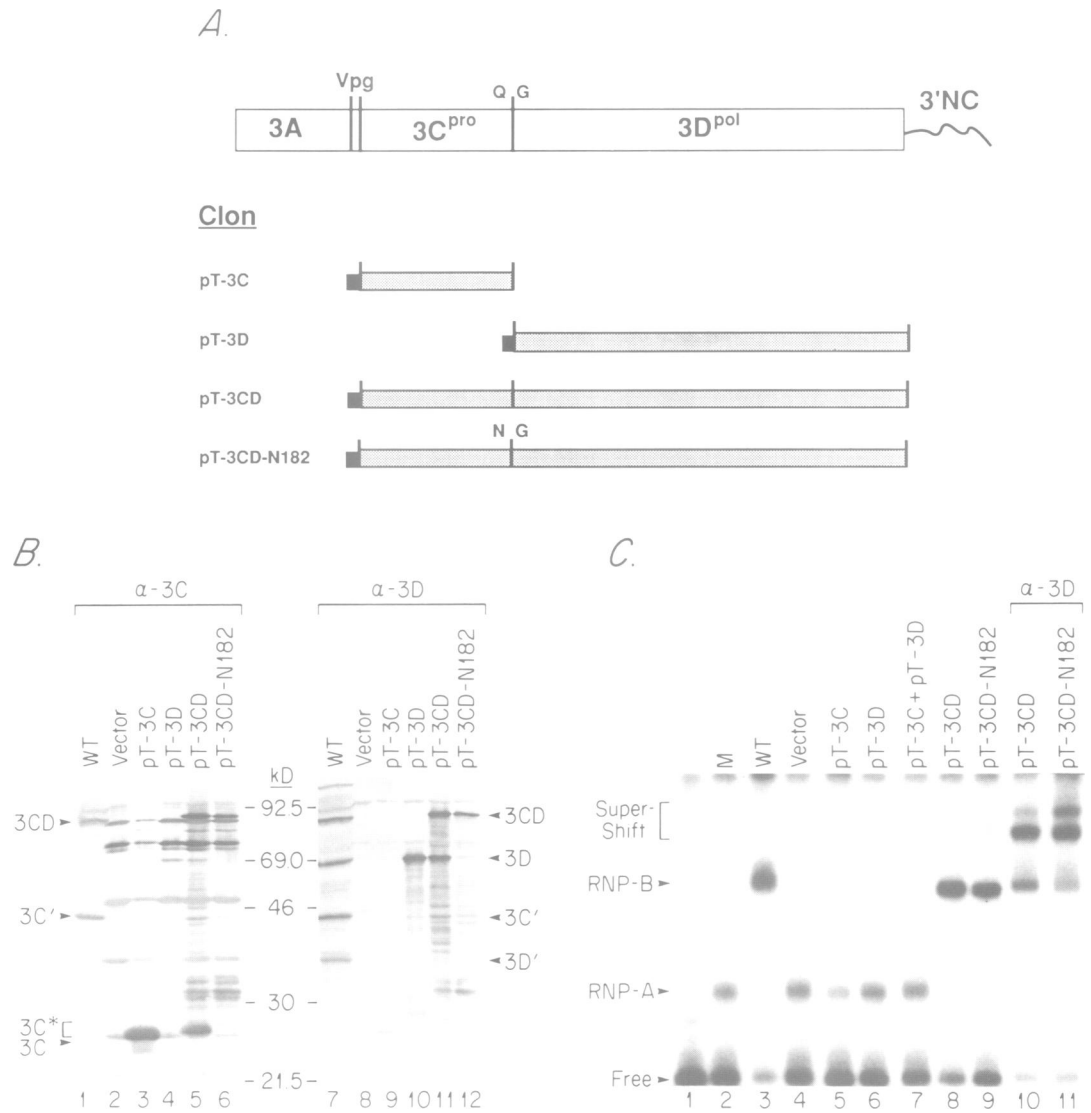

Fig. 2. Expression of poliovirus proteins in *E.coli* and their ability to form complex B. (**A**) Schematic diagrams of various viral proteins expressed in bacteria. The open box represents the P3 region of poliovirus genome, showing the relative position of viral genes. At the junction between $3C^{pro}$ and $3D^{pol}$, the dipeptide corresponding to the proteolytic cleavage site (Q-G) is indicated. The shaded boxes indicate the portions of the poliovirus genome cloned into the T7 expression vector to generate clones that code for $3C^{pro}$, $3D^{pol}$, 3CD and 3CD mutated at the proteolytic site (Q-G to N-G). Seven amino acids (M-A-S-G-T-M-D), derived from the vector, are present at the N termini of the recombinant proteins (as indicated by the black box). (**B**) Western blot detection of poliovirus proteins produced in bacteria. Five μl of each crude extract were fractionated by SDS−PAGE, transferred to nitrocellulose membranes, and probed with anti-$3C^{pro}$ or anti-$3D^{pol}$ sera as indicated. Lanes 2 and 8 correspond to extracts of bacteria transformed with the T7 expression vector coding for non-poliovirus proteins. Lanes 1 and 7 contain 5 μl of poliovirus-infected HeLa cell extract. The molecular weights and the positions of specific poliovirus proteins present in infected extracts are indicated. *E.coli*-expressed $3C^{pro}$ (indicated as 3C*), migrates slightly more slowly than normal $3C^{pro}$, possibly due to the additional amino acids present at the N termini. (**C**) RNA binding analysis of proteins produced in bacteria. Uniformly labeled cloverleaf RNA (20 000 c.p.m./ng) was incubated with 2 μl of each extract, as indicated along the top of the panel. Samples were separated by electrophoresis through a native polyacrylamide gel in 0.5 × TBE buffer, and autoradiographed. Lane 1 contains extract buffer, lanes 2 and 3 contain mock- or poliovirus-infected HeLa cell extracts, respectively. Lanes 4−11 contain, in addition to the specific bacterial extract used in each lane (as indicated on top), 2 μl of mock-infected HeLa cell cytoplasmic extract. The reaction in lane 7 was performed with 2 μl of pT-3C extract plus 2 μl of pT-3D extract. Lanes 10 and 11 show similar binding reactions to those in lanes 8 and 9, but containing antisera against $3D^{pol}$ (α-3D).

ribosomal pellet was washed with 0.5 M KCl solution and the material released from ribosomes by the high salt treatment was fractionated by standard chromatography steps (see Materials and methods). This partially purified material contained four major polypeptides as indicated by SDS−PAGE analysis (Figure 3B). Fractions of a similar SDS−PAGE lane were obtained. The proteins were eluted and then renatured, and the activity of these fractions to stimulate RNP-B complex formation was tested by EMSA. The activity was present in a fraction corresponding to a molecular weight of ~36 kDa, suggesting that a single polypeptide of 36 kDa (p36) is the cellular component of the ribonucleoprotein complex B. Further characterization of p36 will be reported independently.

Interaction of p36 with the cloverleaf RNA

To investigate in greater detail the interaction of the host factor with the RNA, we performed RNA footprinting analyses. Cloverleaf RNA was treated with RNase T1 or T2, or irradiated with UV in the presence or absence of a

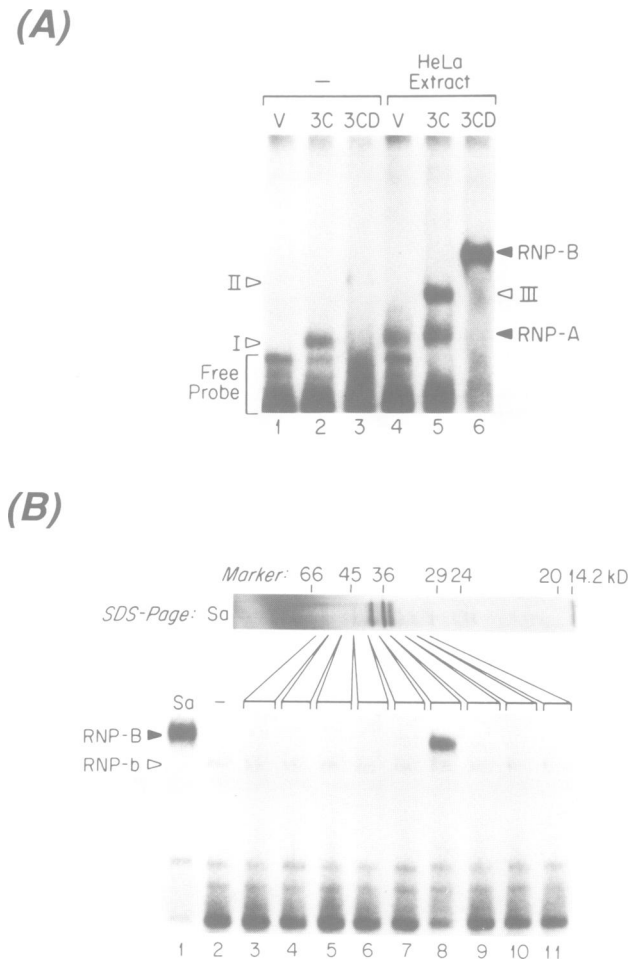

Fig. 3. A cell host factor of 36 kDa is needed for viral complex formation. (**A**) Effect of HeLa cell cytoplasmic extract on the ability of *E.coli*-expressed poliovirus specific proteins to bind to the cloverleaf RNA. In each set of three lanes, bacterial extracts (20 μl) expressing no viral proteins (V), the viral protease, $3C^{pro}$ (3C) or 3CD were incubated with radiolabeled cloverleaf RNA (20 000 c.p.m./ng), in the absence (lanes 1–3) or presence (lanes 4–6) of 4 μg of mock-infected HeLa cell extract. Binding reactions were analysed by electrophoresis through a 5% polyacrylamide native gel. The complexes previously described (RNP-A and RNP-B) are identified by dark arrows, and three new complexes (I, II and III) by open arrows.
(**B**) Denaturation–renaturation identification of the size of the cellular factor. A partially purified fraction of p36 (~2 ng) was analyzed by SDS–PAGE and the gel was silver stained (upper part of the figure). A lane, run in parallel (~200 ng), was cut in slices, proteins were eluted from each fraction and their activity to stimulate complex RNP-B formation was tested by the electrophoretic mobility shift assay. Lanes 1–11 contained 2 μl of bacterial extract expressing 3CD (see Figure 2) and 15 000 c.p.m. of radiolabeled cloverleaf probe in a typical binding reaction. In lane 1, 0.5 μg (5 μl) of partially purified host cell factor was added to the reaction; lane 2 contains 5 μl of elution buffer. Lanes 3–11, 5 μl of eluted material corresponding to each gel slice, as indicated in the diagram, was added to the binding reaction. Complex RNP-B and complex II (named RNP-b in this figure) are indicated at the left.

partially purified fraction containing the cellular host factor. The treated RNA was then analyzed by primer extension. As previously shown, two major RNase-hypersensitive regions could be detected within the cloverleaf structure, at nucleotide numbers 21–25 and 63–67, corresponding to the loops in stem–loop b and stem–loop d, respectively (Figure 4A, lanes 5, 8, 9 and 12; Andino *et al.*, 1990a). The presence of p36 specifically protected the top of

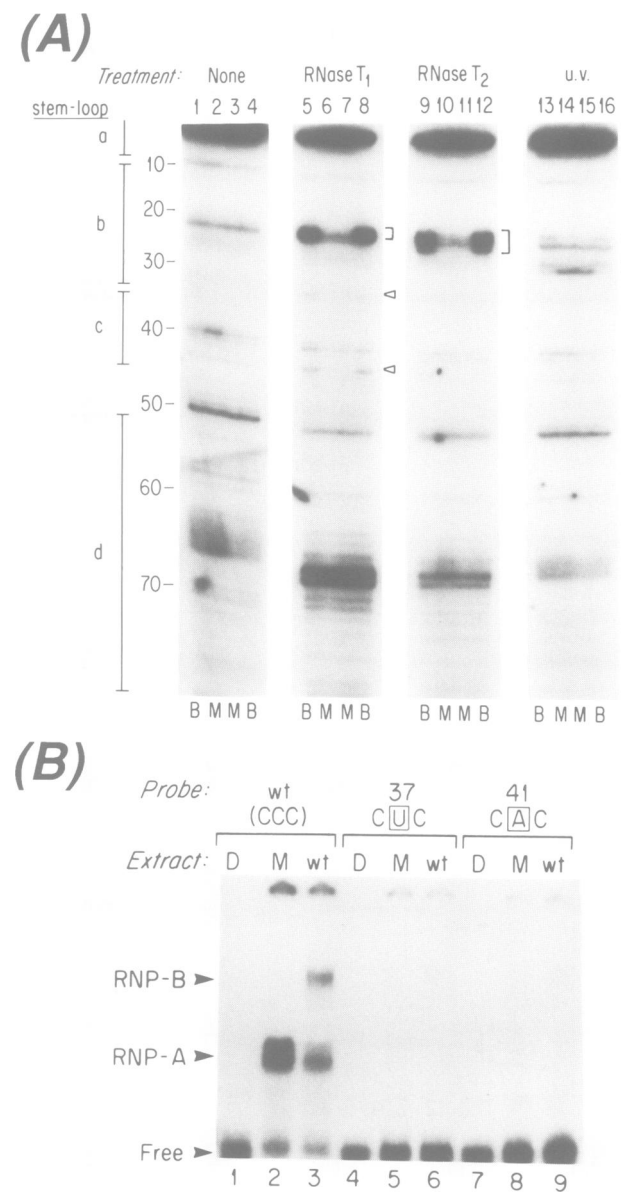

Fig. 4. p36 interacts with the top of stem–loop b of the cloverleaf RNA to form cellular and viral ribonucleoprotein complexes. (**A**) RNA footprinting analysis of the interaction of p36 with the cloverleaf RNA. Binding reactions were performed as described in Figure 2 with unlabeled 5′ cloverleaf RNA (0.5 μg) and 2 μg of BSA (B, lanes 1, 4, 5, 8, 9, 12, 13 and 16), or 2 μg of purified fraction of host cell factor (M, lanes 2, 3, 6, 7, 10, 11, 14 and 15). Then, RNase T1 or T2 was added to the reaction (lanes 5–8 and 9–12, respectively), or the binding reaction was irradiated with UV (lanes 13–16). Lanes 1–4 correspond to untreated RNA after binding reaction. Primer extension was performed using a ^{32}P-labeled primer complementary to nucleotides 91–107. Vertical lines on the left indicate regions corresponding to subdomains within the cloverleaf RNA. Brackets indicate the major RNase hypersensitivity zone protected by p36. Arrows point to regions that are differentially modified by the UV treatment in the presence or absence of p36. (**B**) Effect of point mutations within loop b on complexes RNP-A and -B formation. RNA binding reactions were performed as described in Figure 2. In each set of three lanes, the first shows the free probe after incubation with extract buffer (D), the next two show the resulting complexes after incubating in the binding reaction mock- (M) and wild-type-infected (wt) cell extract. Three different probes were used [20 000 c.p.m. (15 000 c.p.m./ng)]. Lanes 1–3, wild-type cloverleaf RNA; lanes 4–6, nucleotide C24 on top of the stem–loop b of the cloverleaf RNA was mutated to U (probe 37); and lanes 7–9, nucleotide C24 mutated to A (probe 41). Bands corresponding to RNP-B, RNP-A and free probe are indicated.

Table I. Site-directed mutagenesis of 3CD

Clone	Wild-type sequence	Mutant sequence	Proteolytic activity	RNA binding activity
pH31A	5525-GUC CAC GAC 30- V H D	5525-GUC GGC GAC 30- V A D	−	−
pD32A	5528-CAC GAC AAC 31- H D N	5528-CAC GGC AAC 31- H A N	+	−
pH40E	5552-ACC CAC GCU 39- T H A	5552-ACC GAG GCU 39- T E A	−	+
pE71Q	5645-CUU GAA AUC 70- L E I	5645-CUU CAA AUC 70- L Q I	−	+
pR84S	5684-UUC AGA GAC 83- F R D	5684-UUC UCU GAC 83- F S D	+	−
pD85E	5687-AGA GAC AUU 84- R D I	5687-AGA GAG AUU 84- R E I	+	−
pR143S	5861-ACC AGA GCA 142- T R A	5861-ACC UCU GCA T S A	+	+
pC147S	5873-CAG UGU GGU 146- Q C G	5873-CAG AGC GGU 146- Q S G	+	+
pG149C	5879-GGU GGA GUC 148- G G V	5879-GGU UGU GUC 148- G C V	−	−
pT154Q	5894-UGU ACU GGG 153- C T G	5894-UGU CAA GGG 153- C Q G	+	−
pG155L	5897-ACU GGG AAA 154- T G K	5897-ACU UUG AAA 154- T L K	+	−
pK156E	5900-GGG AAA GUC 155- G K V	5900-GGG GAA GUC 155- G E V	+	±
pH161N	5915-AUG CAU GUU 160- M H V	5915-AUG AAU GUU 160- M N V	−	+
pA171L	5945-UUU GCA GCG 170- F A A	5945-UUU CUU GCG 170- F L A	−	−
pR176S	5960-AAG CGA UCA 175- K R S	5960-AAG UCC UCA 175- K S S	+	−

Amino acids $3C^{pro}$ that are conserved among enteroviruses were substituted as indicated in the text. The nucleotide numbers correspond to the viral genome positions, whereas the amino acid numbers correspond to their positions within the $3C^{pro}$ protein. Mutated nucleotides and amino acids are underlined. Proteolytic and RNA binding activity for each individual mutated protein were assayed as described in Figure 5.

stem−loop b, nucleotide numbers 21−25, as well as 32 and 43 (Figure 4A, lanes 6, 7, 10 and 11). Consistently, UV photo-crosslinking treatment also indicated that loop b is the target sequence for p36, because two stop points, generated by the UV treatment, at nucleotides 20 and 23, disappeared in the presence of the cellular factor, and a new strong band appeared at position 24, perhaps due to photo-crosslinking between nucleotide C24 and the host factor (Figure 4A, lanes 14 and 15).

To confirm that the cellular factor interacts with sequences present within stem−loop b, point mutations were introduced in loop b by changing nucleotide C24 to either U or A. As expected, the ability of mutated RNA probes to form ribonucleoprotein complexes with uninfected and infected HeLa cell extract were strongly reduced (Figure 4B, lanes 5, 6, 8 and 9). Furthermore, poliovirus mutants carrying these alterations showed a reduction in viral replication rate (the size of mutant plaques are 20−40% smaller than wild-type plaques, data not shown). This confirms that sequences present at the top of stem−loop b of the cloverleaf structure are important determinants for complex formation and that the complex observed in uninfected cell extracts is due to the interaction of p36 at the top of the stem−loop b of the cloverleaf.

The RNA binding domain in 3CD viral protein

In previous studies, we have shown that a four-base insertion mutant mapping at the top of stem−loop d of the cloverleaf RNA can be suppressed by alteration of the amino acid sequence of the viral protease $3C^{pro}$, suggesting that $3C^{pro}$ carries important determinants for RNA binding. $3C^{pro}$ by itself, however, was a poor RNA binding protein (Figure 2C, lane 5). A weak affinity for RNA was manifested by $3C^{pro}$ using 10 times more *E.coli*-expressed protein; complexes denoted I and III were formed in the absence and presence of p36, respectively (Figure 3A, lanes 2 and 5). Complex I appeared to be formed by direct interaction of $3C^{pro}$ with the cloverleaf RNA because no such complex was observed when bacterial extract containing non-poliovirus proteins was used in the binding reaction (Figure 3A, lane 1). Complex III, migrating with an electrophoretic mobility intermediate between RNP-A and RNP-B, is probably the result of both $3C^{pro}$ and p36 interacting with the RNA (Figure 3A, lane 5). Thus, the poliovirus $3C^{pro}$ protease seems to be both a proteinase and an RNA binding protein.

To confirm and extend these observations, we generated several 3CD mutants by alteration of the most conserved amino acids of $3C^{pro}$ (Table I). Mutated 3CD was produced

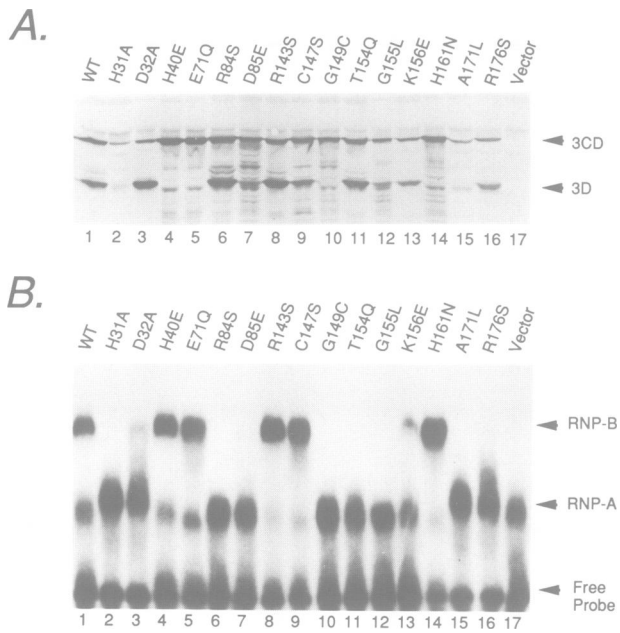

Fig. 5. Mapping RNA binding domain within 3CD by site-directed mutagenesis. Some of the most conserved amino acids within $3C^{pro}$ were mutated (see Table I) and the ability of the altered protein to undergo autoproteolytic processing and to interact with the cloverleaf RNA was analyzed. Lane 1 corresponds to wild-type 3CD, and lane 17 contains bacterial extract transformed with T7 expression vector. (**A**) A Western blot of bacterial extracts expressing mutated 3CD was probed with anti-3D rabbit serum. Arrows indicate bands corresponding to 3CD and to $3D^{pol}$. (**B**) RNA binding reactions were performed as described in Figure 2. All reactions mixed contained 2 μl of crude mock-infected cytoplasmic HeLa cell extract, and wild-type cloverleaf RNA was used as a probe. Complexes RNP-A and RNP-B are indicated.

in *E.coli*, and tested for its ability to act as protease and as an RNA binding protein. $3C^{pro}$ and $3D^{pol}$ are generated in the bacterial expression system by self-cleavage of 3CD, just as they are in poliovirus-infected cells (Krausslich and Wimmer, 1988). Thus, to measure the proteolytic activity of the mutated 3CD, we analyzed the bacterial extracts by Western blot using anti-$3D^{pol}$ serum. The presence of a band corresponding to $3D^{pol}$ indicated that a given 3CD mutant was still active as a protease in the auto-processing reaction. In parallel, the RNA binding activity of each mutated 3CD protein was investigated using the electrophoretic mobility shift assay.

Escherichia coli extracts expressing wild-type 3CD have both protease and RNA binding activities as indicated by the presence of a band corresponding to $3D^{pol}$ in the Western blot (Figure 5A, lane 1) and the formation of complex B in the binding reaction (Figure 5B, lane 1). Alterations of amino acids in $3C^{pro}$ yielded three kinds of mutants, those with very low or undetectable proteolytic activity but normal complex B formation (H40E, E71Q, H161N; Figure 5A and B, lanes 4, 5 and 14, respectively), those which bound poorly to the cloverleaf RNA but displayed normal proteolysis (D32A, R84S, D85E, T154Q, G155L, K156E and R176L; Figure 5A and B, lanes 3, 6, 7, 11, 12, 13 and 16, respectively), and those which lost both activities (H131A, G149C and A171L; Figure 5A and B, lanes 2, 10 and 15, respectively). The last group may represent ones where the alterations severely modified the entire protein structure and consequently we did not attempt to draw any conclusions about the domain affected by these mutations. In contrast, mutations that affect only proteolytic processing or RNA binding activity we interpret to represent specific disruption of the proteolytic pocket or RNA binding domain, respectively, and therefore permit the tentative identification of such functional domains.

Phylogenic comparisons and computer structure modeling indicate that $3C^{pro}$ poliovirus protease belongs to a large group of serine proteases such as mammalian chymotrypsin or bacterial α-lytic proteinase (Bazan and Fletterick, 1988; Gorbalenya *et al.*, 1989), although the essential nucleophile is a cysteine in the poliovirus enzyme. Recently, the X-ray structure for a closely related serine protease, Sindbis virus core (SVC) protein, has been obtained (Choi *et al.*, 1991). The SVC polypeptide is folded into two similar 'Greek key' β-barrel domains (Figure 6, in green and red) connected by a bridge of ~27 amino acids (in dark blue) with the substrate site situated between the β-barrel domains.

Using the SVC structure as a model, we have mapped all of the mutants that caused a loss of only a single function of $3C^{pro}$ onto their equivalent positions in the structure. Mutations affecting only proteolytic processing activity mapped within the proposed catalytic pocket between the two β-barrel domains (Figure 6, light blue), whereas those that disrupted complex B formation mapped on the opposite face of the protein, although they involve amino acids that form parts of three independent loops and the connector bridge (in yellow).

A poliovirus subgenomic replicon carrying a luciferase reporter gene allows the physiological analysis of non-viable mutants

Lethal mutations for poliovirus have been difficult to study under physiological conditions due to the lack of a sensitive method of analysis. Because many of the alterations introduced within the cloverleaf structure or the $3C^{pro}$ gene lead to the generation of non-viable viruses, we developed an assay which permits the analysis of this type of mutant.

It has been reported that a large portion of the RNA encoding for capsid proteins is not required for viral RNA replication (Kaplan and Racaniello, 1988; Hagino-Yamagishi and Nomoto, 1989) and it can be replaced by a reporter gene without major consequences for RNA synthesis (Percy *et al.*, 1992). The expression of a reporter gene should be proportional to the amount of viral RNA present in the cell, and therefore should act as a measure of viral RNA synthesis. We replaced the viral RNA encoding the structural proteins by the *Photinus pyralis* firefly luciferase gene (de Wet *et al.*, 1987), and an artificial cleavage site for the viral protease $2A^{pro}$ was engineered at the 3′-end of the reporter gene (Figure 7A). In this way, translation of the subgenomic replicon RNA would generate a polyprotein containing luciferase at its N terminus, but appropriate proteolytic processing by $2A^{pro}$ would release the active enzyme from the rest of the polyprotein and normal viral RNA replication could proceed.

We first measured the levels of RNA accumulated after transfection with luciferase chimeric subgenomic replicon (RLuc-31) and wild-type full-length poliovirus RNA. HeLa cells were transfected with *in vitro* synthesized RNA, and at several times post-transfection cell lysates were obtained

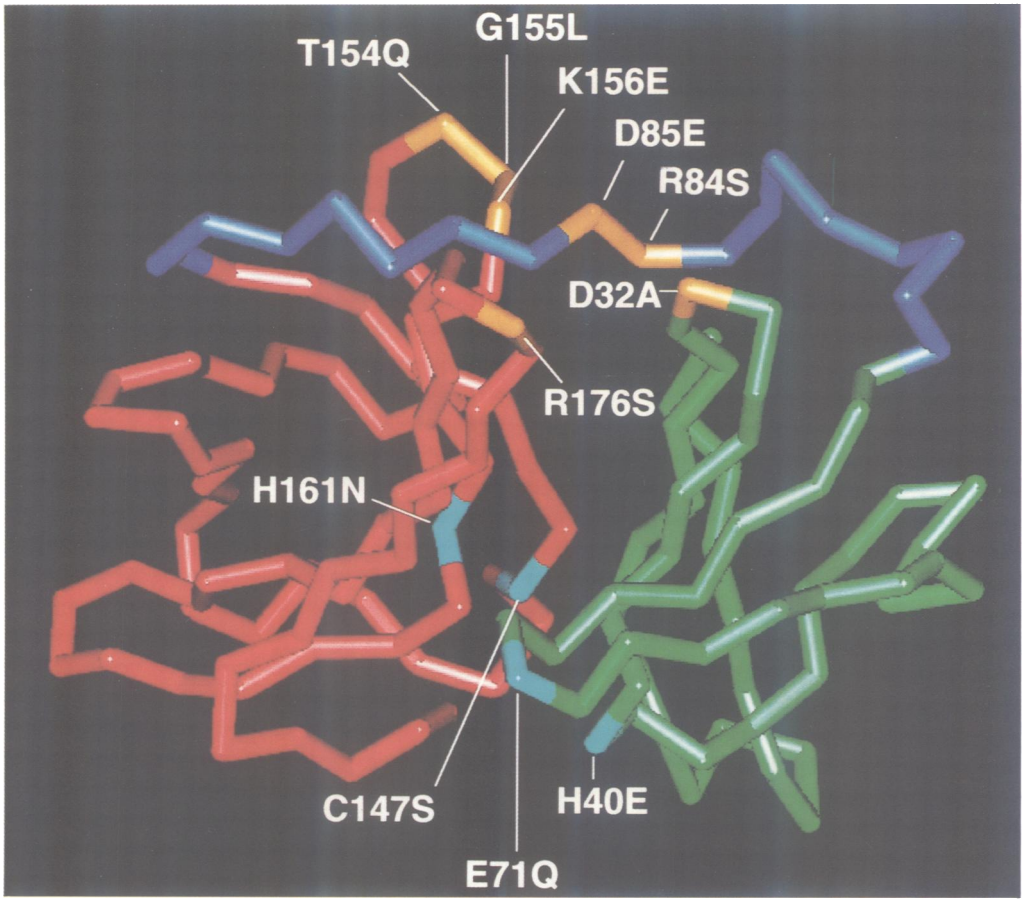

Fig. 6. Plotting results of the 3CD mutagenesis analysis on a three-dimensional structure model of $3C^{pro}$ reveals two well-defined domains: a proteolytic pocket and an RNA binding domain. The structure of the closely related protein Sindbis virus core protein (SVC) is shown. The polypeptides fold into two similar 'Greek key' β-barrel domains (in green and in red) connected by a bridge (in dark blue). Mutated amino acids that affect autoproteolytic processing are indicated in light blue, and those disrupting RNP-B complex formation are in yellow.

and both luciferase activity and viral RNA levels were determined. RNase protection assays indicated that RLuc-31 replicates its RNA with similar kinetics to full-length poliovirus during the first 8 h post-transfection (Figure 7B). By 10 h post-transfection, the amount of wild-type viral RNA accumulated was twice that of the subgenomic replicon; this effect most likely reflects the relative instability of unpackaged RNA from the subgenomic replicon when cell death begins. Luciferase activity detected at different time points post-transfection correlated with the levels of RNA accumulated (Figure 7C). This suggests that the enzymatic activity actually reflects the accumulation of the replicon mRNA; therefore, estimation of luciferase activity can be an accurate and sensitive measure of the RNA replication of the subgenomic replicon. Because luciferase is an unstable enzyme *in vivo* (only 10% of the untreated control activity remains after 2 h of cycloheximide treatment; data not shown), the enzymatic activity must reflect the steady-state level of RNA at any particular time.

The accumulation of luciferase activity during RLuc-31 replication, when analyzed on a semi-logarithmic scale, showed three phases. Luciferase activity increased during the first hour post-transfection, followed by a 2 h plateau, then increased exponentially during the final 4–5 h of the assay (Figure 7D). The last phase of the curve corresponds to the exponential increase of viral RNA as measured by RNase protection (Figure 7B); the early phase of luciferase accumulation must then reflect translation of the input RNA.

Subgenomic luciferase replicons carrying lethal mutations within the 5′ non-coding region or viral proteins were constructed. Mutations that affect RNP-B complex formation by disrupting the cloverleaf structure (RLuc-61 and RLuc-72) or the $3C^{pro}$ RNA binding domain (RLuc-181) exhibited the early but not the late increase in luciferase activity. Activity remained constant for 9 h, indicating that these mutations do not alter either translation ability or stability of the RNA. But the lack of the later exponential increase suggests that the primary defect of these mutants is in RNA synthesis. As a control, a one amino acid insertion mutant defective in the elongation activity of the RNA polymerase (RLuc-56; Burns *et al.*, 1989; R.Andino and D.Baltimore, unpublished results) and a mutant containing a point mutation within the $3C^{pro}$ gene that abolishes protease activity, were analyzed using our replicon system. Both mutants showed similar characteristics, yielding only the early increase in luciferase activity, which agrees with a primary defect in RNA replication. As expected, mutations mapping within the part of the 5′ non-coding region involved in translation of the RNA did not generate any luciferase activity. Thus, the analysis of lethal mutants affecting complex RNP-B

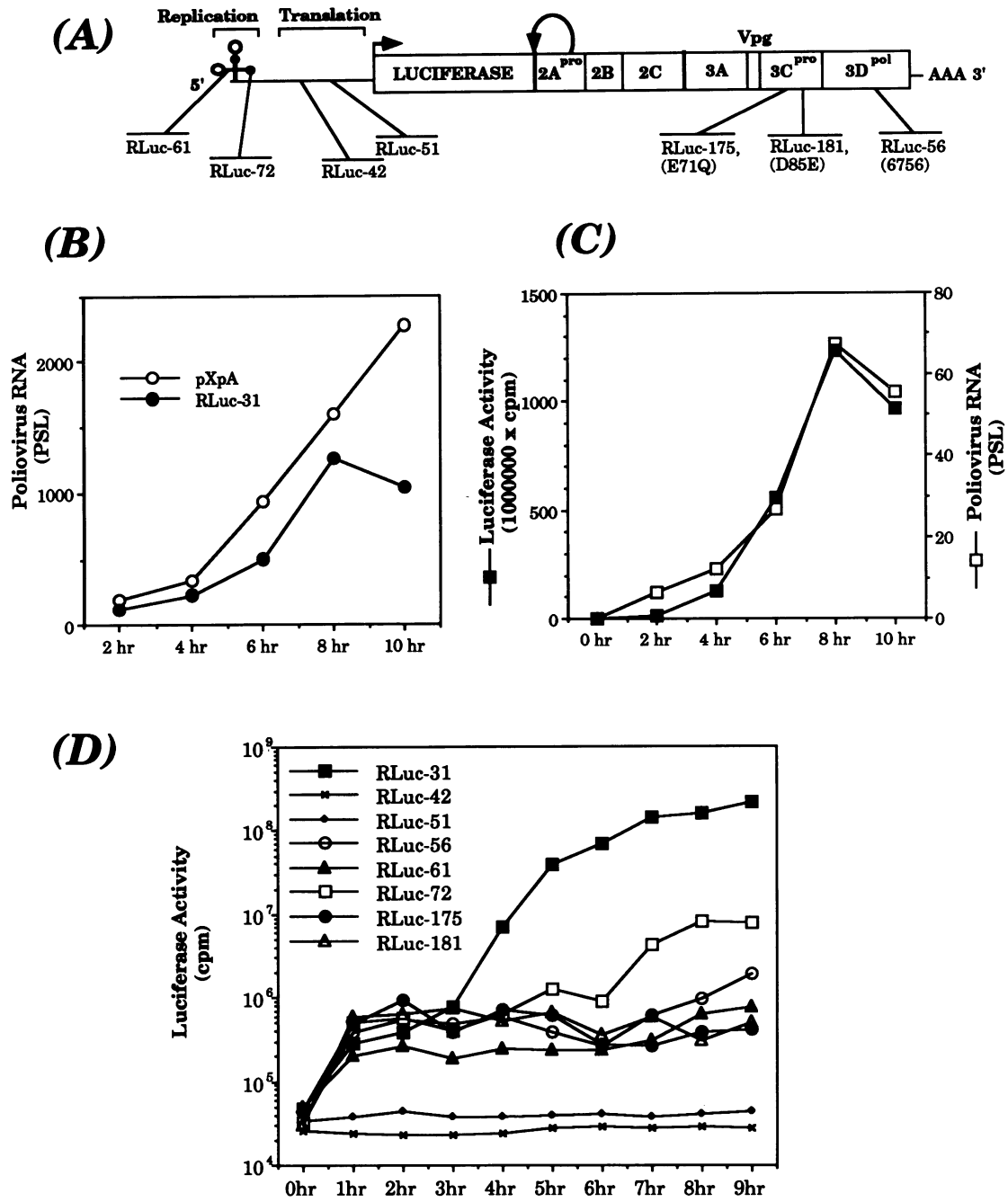

Fig. 7. Analysis of a subgenomic replicon carrying the luciferase gene reveals that complex RNP-B is primarily involved in RNA synthesis. (**A**) Schematic representation of the genome of a chimeric poliovirus replicon. A bar represents the open reading frame and the relative positions of poliovirus and the luciferase gene. Between luciferase and $2A^{pro}$, a recognition and cleavage site for $2A^{pro}$ has been introduced and the proteolytic processing at this site is represented by an arrow. Relative positions of mutations are indicated by lines that end with the corresponding mutant name. Replication and translation regions at the 5′ non-coding region are indicated by keys. (**B**) Accumulation of viral RNA after transfection with full-length and replicon RNA. At various times post-transfection, total RNA from transfected HeLa cells was obtained and levels of specific viral RNA were assayed by RNase protection with an antisense probe corresponding to the 2A gene region. The protected probe was analyzed by 8% urea–PAGE, and the specific band was quantitated by a Bio-Imaging Analyser apparatus (Fujix Bas 1000). PSL is equivalent to d.p.m. (**C**) Comparison of viral RNA and luciferase activity produced at various times post-transfection with the wild-type luciferase subgenomic replicon (RLuc-31). Viral RNA accumulation was determined as in (B). Luciferase activity was measured from the same extracts before phenol extraction and normalized for protein concentration. (**D**) Luciferase activity produced by wild-type and several mutants of the chimeric luciferase replicon after RNA transfection in HeLa cell. Enzymatic activity was estimated as in (C) and is expressed on a logarithmic scale. The symbols utilized to identify each mutant are shown within the figure.

formation indicates that the complex is primarily involved in RNA synthesis, but does not affect translation or stability of the RNA.

Discussion

These data show that the previously identified RNP-B complex that forms around the 5′-terminal 100 nucleotides

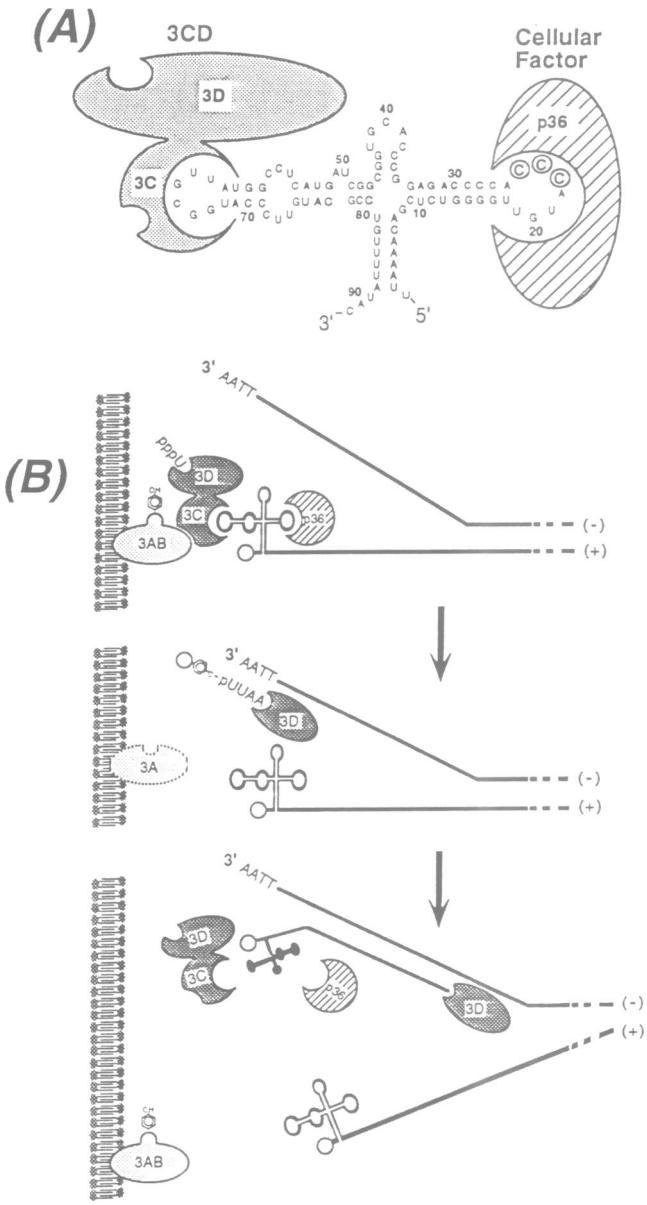

Fig. 8. A model for poliovirus RNA synthesis: the trans-initiation mechanism. (**A**) Scheme of the structure of the complex RNP-B. Viral factor 3CD and cellular factor p36 are shown interacting with their specific target sequences. Three cytosines phylogenetically conserved and important for p36 binding are indicated by circles. For 3CD, the RNA binding domain and the proteolytic pocket are shown on opposite sides of 3C; the pocket in the 3D domain represents a putative nucleotide binding site of the RNA polymerase. (Note: the representation of the cloverleaf RNA is inverted from its conventional form to facilitate comparison with part B of the figure.) (**B**) Three initial postulated steps of poliovirus plus strand RNA synthesis. The upper picture represents a negative strand (−) acting as a template and a resident positive strand (+) holding the initiation complex consisting of the 5′-cloverleaf RNA, 3CD, p36 and—also attached to the membrane—the 3AB precursor of the primer peptide (Vpg). It is suggested that 3CD acts in three ways in the complex: addition of one or two U residues to 3B (Vpg), cleavage of 3B from 3A and cleavage of itself to yield 3C and 3D. The middle picture shows the progress of the reaction after Vpg-pU(pU) is used as a primer for 3D to begin the elongation reaction. Note that after 3CD is auto-proteolytically processed complex RNP-B disassembles. The bottom picture shows that after 3D has synthesized at least the first 100 nucleotides of poliovirus genomic RNA a new cloverleaf structure will form, allowing the formation of a new RNP-B complex that can then catalyze the initiation of the next plus strand RNA.

of poliovirus RNA involves two proteins: the uncleaved 3CD viral protease-polymerase precursor and a ribosome-associated cellular p36. The p36 appears to have binding contacts near the unpaired nucleotides of stem−loop b while genetic experiments had placed important 3CD contacts near the loop of stem−loop d (Andino *et al.*, 1990a,b), suggesting that each protein has a separate binding region within the cruciform structure of the 5′ terminus (Figure 8A). The 3C protease is able to interact weakly with the RNA, and several amino acids probably involved in binding were identified by mutagenesis. Using the structure of a related protein as a guide, we propose an RNA binding site on 3C located on a side opposite from the protease active site.

To probe the physiological role of RNP-B, a subgenomic replicon expressing luciferase was used. Mutations that affect RNA−protein interactions of complex B were introduced into the genome of the replicon. These mutations completely abolished RNA replication without affecting RNA translation or stability.

Structure of 3C and the formation of RNP-B

We have demonstrated that major determinants for RNA binding reside within the $3C^{pro}$ protease; however, the affinity of the uncleaved precursor 3CD for the cloverleaf RNA is ~10 times higher than that of $3C^{pro}$ alone. Two possibilities to explain this effect are that either the RNA polymerase $3D^{pol}$ may interact with RNA and help stabilize the RNP-B complex or the $3D^{pol}$ segment of 3CD might change the conformation of the RNA binding domain in $3C^{pro}$ so as to increase its affinity. In either case, it is clear that the precursor 3CD is the viral RNA binding protein *in vivo*. The relative affinities for RNA suggest that upon proteolytic processing of 3CD, the RNP-B complex may disassemble. This might contribute to regulation of the particular replication step that is catalyzed by the ribonucleoprotein complex.

It is clear that $3C^{pro}$ is both an RNA binding protein and a protease. The RNA binding domain of $3C^{pro}$ does not seem to belong to other previously described RNA binding families of cellular proteins, and may represent a new class of RNA binding proteins. Interestingly, Sindbis virus core protein, a serine protease, is also an RNA binding protein that interacts specifically with the 49S genomic RNA to form the icosahedral nucleocapsid (Geigenmuller *et al.*, 1993). This suggests that RNA binding activities may be found in other viral proteases as well.

The formation of RNP-B depends on a cellular protein of 36 kDa, but it is not clear at this point whether p36 enhances the RNP-B complex formation because it induces a conformational change in the RNA target sequence, or because it stabilizes 3CD binding through protein−protein interactions. The binding of p36 requires specific nucleotides present on the top of stem−loop b of the poliovirus cloverleaf RNA (Figure 8A). Phylogenetic comparisons show that these three cytosines are well-conserved among enteroviruses, suggesting that this group of viruses shares the requirement for the same cellular factor. Because of the high mutational rate and plasticity of the poliovirus genome, one might expect that 3CD and a cloverleaf RNA target could co-evolve to interact efficiently by themselves. The fact that p36 is required suggests that the cellular factor may have not only a structural role but also a functional role in catalysis.

A large proportion of the total cellular p36 is found in the ribosomal fraction. It seems reasonable that cytoplasmic RNA virus might recruit necessary factors for its own replication from the largest RNA–protein complex present in the cytoplasm, the translation machinery. In this regard, it is perhaps relevant that Qβ, an RNA phage, utilizes an RNA polymerase complex consisting of a phage-encoded polypeptide and three bacterial proteins which normally are involved in the translation of cellular mRNA (for review see Biebricker and Eigen, 1988). Because the RNP-B complex seems to be involved in initiation of polioviral RNA synthesis, the strategy of RNA replication used by both animal RNA viruses and bacterial phages might share a common feature.

A model of poliovirus RNA chain initiation

We have previously shown that mutations that disrupt complex RNP-B formation reduce the amount of viral plus strand RNA accumulated during viral replication (Andino *et al.*, 1990a). In this report we have shown that mutants that disrupt RNP-B are able to translate their RNA at wild-type levels, and that RNA stability is unaffected. Therefore, lethal mutations disrupting complex B formation must primarily affect RNA synthesis. Because the poliovirus RNA polymerase by itself is able to elongate non-specific RNA templates, the requirement for RNP-B must be at the initiation of positive strand RNA synthesis.

As mentioned above, poliovirus RNA polymerase is a primer-dependent enzyme. The covalent linkage of Vpg to nascent strands of viral RNA suggests that the 22 amino acid Vpg acts as the primer with the hydroxyl group of a tyrosine residue accepting the first U residue (Wimmer, 1982). The accumulation of Vpg-pU(pU) in poliovirus-infected cells suggests that initiation of RNA replication might first involve the synthesis of this structure, perhaps without a template [there is evidence that the first U is not templated (Harmon *et al.*, 1991)] followed by subsequent elongation to form larger viral RNA molecules. Strong evidence for the primer role was provided by Takegami *et al.* (1983) who showed that labeled Vpg-pU(pU) could be chased into poliovirus RNA molecules. Much of Vpg, also called 3B, is found in cells as a part of a precursor, 3AB. 3AB is tightly associated with membranes because of the highly hydrophobic nature of 3A. The entire viral replication machinery appears to be linked to membranes and viral RNA synthesis is detergent sensitive, indicating the critical role that membranes play in RNA replication.

Based on these structural and functional findings, we propose a model for the initiation of poliovirus RNA synthesis (schematized in Figure 8B). In this model, the reaction is initiated by binding of the viral factor (3CD) and the cellular protein (p36) to the cloverleaf RNA structure at the 5′-end of the genomic RNA. Thus, this structure represents the poliovirus genome initiation complex. Because the ribonucleoprotein complex contains the viral protease ($3C^{pro}$) and the viral RNA polymerase ($3D^{pol}$), the proteolytic processing of 3AB and the uridylylation of Vpg could be directly catalyzed by these enzymes within the context of the complex. It has been shown that the 3AB is cleaved to 3A and 3B by $3C^{pro}$ (for review see Krausslich and Wimmer, 1988), and there is genetic evidence suggesting that uridylylation of Vpg is catalyzed by $3D^{pol}$ (Toyoda *et al.*, 1987). Thus, $3C^{pro}$ may interact simultaneously with the cloverleaf RNA and with Vpg precursor (3AB) to ensure the local production of Vpg-pU(pU).

After Vpg-pU(pU) has been generated, 3CD may autoproteolytically process itself, inducing disassembly of the complex, thus freeing $3D^{pol}$. The free viral RNA polymerase then may elongate the locally produced primer, Vpg-pU(pU). Finally, once $3D^{pol}$ has transcribed the portion of the 5′ non-coding region corresponding to the cloverleaf structure, a new complex may be built on the 5′-end of the newly synthesized strand and, in turn, this new complex could catalyze the subsequent initiation of the synthesis of the next plus strand RNA.

There are many details to the initiation process that remain obscure, but the use of a ribonucleoprotein complex formed around one end of one nascent RNA molecule to initiate synthesis of the next would represent a new mechanism for the initiation of nucleic acid synthesis. It might seem that such a mechanism would represent a problem for the first molecule to be made on a new replication complex, but it is important to remember that even the first strand of RNA to enter a cell has the initial 100 nucleotide cloverleaf and that minus strand templates are formed by copying plus strands so that RNP-B is always potentially present to catalyze the synthesis of the next strand. This mechanism could be applicable only to plus strand synthesis; there is abundant evidence that minus strand initiation is carried out in an entirely different fashion (Kirkegaard, 1992).

Materials and methods

Cell culture, viral transfection and infection, [^{35}S]Met labeling and cytoplasmic extract preparation

HeLa cells were grown as previously described (Bernstein *et al.*, 1985). HeLa cells on 100 mm dishes were transfected with 1–10 μg of *in vitro* transcribed full-length poliovirus RNA, using the DEAE–dextran procedure (Luthman and Magnusson, 1983). Mutated RNA was sequenced by RNA dideoxy sequencing before transfection. For HeLa cell infection and viral protein labeling, 100 mm Petri dishes containing 3×10^6 cells were uniformly infected using poliovirus at a multiplicity of infection (m.o.i.) of 10, and the cells were incubated at room temperature for 30 min to allow virus to adsorb. Cells were washed once with phosphate-buffered saline solution (PBS), and then covered with 10 ml of Dulbecco's modified Eagle's medium (DME) supplemented with 7% fetal calf serum and incubated at 37°C for 2 h. Then the medium was removed, the cells were washed with PBS and methionine-depleted DME containing 25 μCi of [^{35}S]methionine per ml was added. After 60 min of incubation, cells were washed with cold PBS, resuspended in 1 ml of PBS, transferred to an Eppendorf tube, and collected by centrifugation. Cells were resuspended in 400 μl of buffer H [buffer H: 10 mM HEPES, pH 7.9, 10 mM KCl, 1.5 mM $MgCl_2$, 1 mM DTT, 1% Triton X-100, and 0.1 mM phenylmethylsulfonyl fluoride (PMSF)]. Nuclei were removed by centrifugation and the postnuclear supernatant was centrifuged for 15 min at 150 000 *g*.

RNA binding assays and complex RNP-B isolation

RNA binding reactions and electrophoretic mobility shift assays (EMSA) were performed as previously described (Andino *et al.*, 1990a). The RNA probe was a T7 RNA polymerase transcript, uniformly ^{32}P-labeled, representing the first 108 nucleotides of the poliovirus genomic RNA; occasionally, a mutated RNA probe was obtained as previously described (Andino *et al.*, 1990a) and used as indicated in Figure 4B.

To isolate complex RNP-B containing ^{35}S-labeled proteins, binding reactions were performed as described above, using 100 μl of ^{35}S-labeled cytoplasmic extract in the presence or absence of 5 μg of unlabeled cloverleaf RNA, in a 400 μl reaction volume. A preparative native polyacrylamide gel was submitted to electrophoresis for 12 h at 150 V; the piece of gel containing complex B was isolated and proteins were eluted by passive diffusion in elution buffer [50 mM Tris–HCl, pH 7.5, 2 mM DTT, 0.1 mg/ml bovine serum albumin (BSA), 0.15 M NaCl, 0.1% SDS and 0.1 mM EDTA]. Eluted material was acetone-precipitated, resuspended in SDS–PAGE sample buffer, and analyzed by electrophoresis through

10% SDS–polyacrylamide gel. Immunoprecipitation was performed according to standard procedures (Trono *et al.*, 1988), by using rabbit polyclonal poliovirus type 1 antivirion or $3D^{pol}$ (kindly provided by Dr G.Kaplan) antiserum.

Expression of poliovirus proteins in E.coli

We used the T7 expression system (Rosenberg *et al.*, 1987) to produce various poliovirus proteins used in the experiments described. Plasmids were constructed by inserting PCR-amplified cDNA, corresponding to $3C^{pro}$, $3D^{pol}$ and 3CD coding regions, in a modified version of the expression vector pAR3090 digested with *Asp*718 and *Bam*HI [this modified vector carries an in-frame polylinker with two new restriction enzyme sites (*Kpn*I and *Xho*I)]. PCR reactions were carried out using three sets of oligonucleotide primers—oligonucleotide 1 and 2, 3 and 4, and 1 and 4—to obtain cDNA coding for $3C^{pro}$, $3D^{pol}$ and 3CD, respectively. Primer 1: 5′-AAT TAA CCC TCA CTA AAG GGT ACC ATG GAT GGA CCA GGG TTC GAT-3′; 2: 5′-TAG TGG ATC CTT ATT GAC TCT GAG TGA A; 3: 5′-AAT TAA CCC TCA CTA AAG GGT ACC ATG GAT GGT GAA ATC CAG TGG-3′; 4: 5′-TAG TGG ATT CTT ACT AAA ATG AGT C.

To produce viral proteins, recombinant T7 expression plasmids were transformed into the *E.coli* strain BL21 (DE3), which contained the T7 polymerase gene under the control of the *lac*UV5 promoter. Overnight culture of freshly transformed bacteria was diluted 1/10, and the culture was grown to $OD_{550} = 0.5$ before IPTG was added to a final concentration of 0.4 mM. The induction was carried out for an additional 2 h. Cells were harvested, washed once with PBS, and resuspended in lysis buffer (10 mM HEPES, pH 7.9, 20 mM KCl, 25 mM EDTA, 5 mM DTT, 0.1 mM PMSF, 1% Triton X-100). The suspension was frozen and thawed three times, sonicated for ~30 s to reduce viscosity, and centrifuged at 150 000 *g* for 15 min to remove debris. Glycerol was added to 20% final concentration and supernatant was stored at −70°C.

For Western blot analysis, 5 μl of bacterial extract was mixed with an equal volume of 2 × SDS–PAGE sample buffer, loaded onto a 10% SDS–polyacrylamide gel, and after electrophoresis, proteins were blotted onto nitrocellulose filters by electrotransfer. The membranes were probed with antisera anti-$3D^{pol}$ and $3C^{pro}$ (a kind gift from Dr Bert Semler) as described (Trono *et al.*, 1988).

The RNA binding analysis of bacterially produced proteins was essentially as described above. The amount of specific poliovirus protein used in each RNA binding assay was normalized from immunoblot analysis.

Purification of host cell factor

Twenty liters of HeLa cell culture (~8×10^9 cells) were collected by centrifugation, washed once with PBS, and the pellet resuspended in 4 packed cell volumes of buffer R (10 mM HEPES, pH 7.9, 20 mM KCl, 5 mM $MgCl_2$, 5 mM DTT, 0.1 mM PMSF, 1% Triton X-100). The suspension was incubated for 20 min on ice and nuclei were removed by centrifugation for 10 min at 6000 *g*. The postnuclear supernatant was loaded onto a 1.5 M sucrose cushion, and a ribosomal pellet was obtained by centrifugation at 200 000 *g* for 5 h (45 000 r.p.m. in a Ti50 rotor, Beckman). The ribosomal pellet was resuspended in 5 ml of high salt buffer H (10 mM HEPES, pH 7.9, 25 mM EDTA, 5 mM DTT, 0.1 mM PMSF, 0.5% Triton X-100, 500 mM KCl), incubated 60 min at 4°C, and ribosomal subunits were removed by centrifugation. The high salt wash supernatant was fractionated sequentially on Sephadex S100 gel filtration, DEAE–Sephadex, and phosphocellulose P11 ion-exchange columns in buffer H with appropriate concentrations of KCl. Fractions of each chromatographic step were assayed for their ability to stimulate *E.coli*-expressed 3CD to form complex RNP-B.

A partially purified active fraction, containing ~20 μg of protein, was precipitated with 5 vol of acetone, and size-fractionated by electrophoresis through an SDS–polyacrylamide gel. The lane was cut into slices and each slice was ground to a pulp. To each ground slice was added 300 μl of elution buffer (50 mM Tris–HCl, pH 7.5, 2 mM DTT, 0.1 mg/ml BSA, 0.15 M NaCl, 0.1% SDS and 0.1 mM EDTA) and protein was eluted for 6 h at room temperature. A volume of 200 μl of supernatant was then precipitated with 5 vol of acetone, the acetone precipitates were washed with methanol, air dried and resuspended in 2 μl of 6 M guanidinium hydrochloride. Then 200 μl of buffer H was added to each fraction, incubated for 15 min at room temperature, and 5 μl of each fraction was assayed for RNA binding activity.

RNA footprinting analysis

RNase T1 and T2 treatment, primer extension and gel electrophoresis were performed as previously described (Black and Pinto, 1989). UV photocrosslinking treatment was carried out essentially according to Garcia-Blanco *et al.* (1989). Unlabeled cloverleaf RNA was *in vitro* synthesized as described above. Binding reactions were performed with 5 μg of partially purified host cell factor (one of the most highly purified fractions), or with 5 μg of BSA, in 50 μl. After RNase or UV treatment, RNA was phenol extracted, ethanol precipitated, and used as template for primer extension.

Site-directed mutagenesis

Mutations in the cloverleaf structure were obtained as previously described (Andino *et al.*, 1990a). To create mutations described in Table I, cDNA coding for 3CD was cloned in pBluescript-SK, and uracil-containing single-stranded DNA was obtained by super-infection with helper phage as described by the manufacturer (Bio-Rad). Standard site-directed mutagenesis was then performed as described (Ausubel *et al.*, 1992). The mutated *Asp*718–*Bam*HI fragments were analyzed by double-stranded DNA sequencing and re-inserted into T7 expression vector to express the entire 3CD mutated proteins in bacteria as described above.

Construction and characterization of luciferase subgenomic replicon mutants

Full-length poliovirus cDNA was modified by deleting the entire region of the cDNA encoding the capsid proteins (nucleotides 756–3371). Between the first and second codon, an in-frame polylinker was inserted containing restriction sites (*Eco*RI and *Not*I) to facilitate the insertion of the luciferase gene. These modifications were performed by a version of the polymerase chain reaction (PCR) known as overlap extension. In brief, two independent PCR reactions were performed using oligonucleotides #1 and #2, and #3 and #4 (listed below) to amplify portions of the poliovirus genome from nucleotides 1–749 and 3371–4040, respectively. The correct PCR product was purified by agarose gel electrophoresis, combined, and a second PCR amplification was performed using oligonucleotides #1 and #4. An ~1400 bp DNA fragment was purified, digested with *Sal*I and *Bst*E2 and ligated to a fragment of ~8600 bp obtained from digesting the full-length poliovirus DNA clone pSR-XpA with the same enzymes. The modified plasmid was further modified by inserting a PCR fragment corresponding to the luciferase gene (amplified with oligonucleotides #5 and #6, this reaction generates *Eco*RI and *Not*I sites at the 5′- and 3′-ends of the fragment, respectively).

Oligonucleotides: 1, 5′-TACG GTC GAC C TAA TAC GAC TCA CTA TAG G. 2, 5′-CTC GAG ACC GCG CGC ACC AGC GGC CGC TCC GAA TTC CTG ACC CAT TAT G; 3, 5′-TAT GAA TTA GGA GCG GCC CGT GGA GCG CGC GGT CTC GAG GAT CTG ACC ACA TAT-3′; 4, 5′-AGC ATC ACA CC AAG AAG-3′; 5, 5′-GGA GCG GCC GCT GAA GAC GCC AAA-3′; 6, 5′-GTG CTC GAG CAA TTT GGA CTT TCC-3′.

To test the replication characteristics of these replicons, 100 mm Petri dishes containing ~3×10^6 HeLa cells were transfected with *in vitro* synthesized RNA as previously described (Luthman and Magnusson, 1983). At different times monolayers were washed with PBS, cells were taken in 1 ml of PBS, concentrated by centrifugation, and the cell pellet lysed in lysis buffer and luciferase activity was measured using a luciferase assay system as recommended by the manufacturer (Promega). Total RNA was extracted by adding 1% SDS final concentration, 1 vol of phenol, followed by ethanol precipitation. RNase protection assay was performed according to Andino *et al.* (1990a). The riboprobe used was an antisense [^{32}P]RNA corresponding to nucleotides 3385–3920 of poliovirus genomic RNA. The product of the RNase protection reaction was resolved in urea–PAGE, and the protected bands were quantified using a Bio-Imaging Analyser (Fujix Bas 1000).

Acknowledgements

We are grateful to Drs Gerardo Kaplan for anti-3D antiserum, Douglas Black for technical advice, and Mark B.Feinberg, Alan Frankel, Laura Baxter and Shelley D.Suggett for their useful comments on the manuscript. This work was supported by Public Health Service grant no. AI22346 to D.Baltimore.

References

Andino,R., Rieckhof,G.E. and Baltimore,D. (1990a) *Cell*, **63**, 269–380.

Andino,R., Rieckhof,G.E., Trono,D. and Baltimore,D. (1990b) *J. Virol.*, **64**, 607–612.

Ausubel,F.M., Brent,R., Kingston,R.E., Moore,D.D., Seidman,J.G., Smith,J.A. and Struhl,K. (eds) (1992) *Current Protocols in Molecular Biology*. Green Publishing Associates and Wiley-Interscience, New York.

Bazan,J.F. and Fletterick,R.J. (1988) *Proc. Natl Acad. Sci. USA*, **85**, 7872–7876.

Bernstein,H.D., Sonenberg,N. and Baltimore,D. (1985) *Mol. Cell. Biol.*, **5**, 2913–2923.
Bernstein,H.D., Sarnow,P. and Baltimore,D. (1986) *J. Virol.*, **60**, 1040–1049.
Biebricker,D.K. and Eigen,M. (1988) In Domingo,E., Holland,J. and Ahlquist,P. (eds), *RNA-directed Virus Replication*. CRC Press, Boca Raton, FL, Vol. 1, pp. 1–18.
Black,D.L. and Pinto,A.L. (1989) *Mol. Cell. Biol.*, **9**, 3350–3359.
Burns,C.C., Lawson,M.A., Semler,B.L. and Ehrenfeld,E. (1989) *J. Virol.*, **63**, 4866–4874.
Choi,H.K., Tong,L., Minor,W., Dumas,P., Boege,U., Rossmann,M.G. and Wengler,G. (1991) *Nature*, **354**, 37–43.
de Wet,J.R., Wood,K.V., DeLuca,M., Helsinki,D.R. and Subramani,S. (1987) *Mol. Cell. Biol.*, **7**, 725–737.
Garcia-Blanco,M.A., Jamison,S.F. and Sharp,P.A. (1989) *Genes Dev.*, **3**, 1874–1886.
Geigenmuller,G.U., Nitschko,H. and Schlesinger,S. (1993) *J. Virol.*, **67**, 1620–1626.
Giachetti,C. and Semler,B.L. (1991) *J. Virol.*, **65**, 2647–2654.
Gorbalenya,A.E., Donchenko,A.P., Blinov,V.M. and Koonin,E.V. (1989) *FEBS Lett.*, **243**, 103–114.
Hagino-Yamagishi,K. and Nomoto,A. (1989) *J. Virol.*, **63**, 5386–5392.
Harmon,S.A., Richards,O.C., Summers,D.F. and Ehrenfeld,E. (1991) *J. Virol.*, **65**, 2757–2760.
Kaplan,G. and Racaniello,V.R. (1988) *J. Virol.*, **62**, 1687–1696.
Kirkegaard,K. (1992) *Curr. Opin. Genet. Dev.*, **2**, 64–70.
Krausslich,H.G. and Wimmer,E. (1988) *Annu. Rev. Biochem.*, **57**, 701–754.
Kuhn,R.J., Tada,H., Ypma-Wong,M.F., Semler,B.L. and Wimmer,E. (1988) *J. Virol.*, **62**, 4207–4215.
Li,J.P. and Baltimore,D. (1988) *J. Virol.*, **62**, 4016–4021.
Luthman,H. and Magnusson,G. (1983) *Nucleic Acids Res.*, **11**, 1295–1308.
Pelletier,J., Kaplan,G., Racaniello,V.R. and Sonenberg,N. (1988) *Mol. Cell. Biol.*, **8**, 1103–1112.
Percy,N., Barclay,W.S., Sullivan,M. and Almond,J.W. (1982) *J. Virol.*, **66**, 5040–5046.
Rosenberg,A.H., Lade,B.N., Chui,D.S., Lin,S.W., Dunn,J.J. and Studier,F.W. (1986) *Gene*, **56**, 125–135.
Sonenberg,N. (1987) *Adv. Virus Res.*, **33**, 175–204.
Takegami,T., Kuhn,R.J., Anderson,C.W. and Wimmer,E. (1983) *Proc. Natl Acad. Sci. USA*, **80**, 7447–7451.
Toyoda,H., Yang,C.F., Takeda,N., Nomoto,A. and Wimmer,E. (1987) *J. Virol.*, **61**, 2816–2822.
Trono,D., Andino,R. and Baltimore,D. (1988) *J. Virol.*, **62**, 2291–2299.
Wimmer,E. (1982) *Cell*, **28**, 199–201.

Received on May 19, 1993